0026-895X/08/7403-544–551$20.00
MOLECULAR PHARMACOLOGY

Mol Pharmacol 74:544–551, 2008
Vol. 74, No. 3
47472/3372215
Printed in U.S.A.

ACCELERATED COMMUNICATION

Ligand-Dependent Oligomerization of Dopamine D_2 and Adenosine A_{2A} Receptors in Living Neuronal Cells[S]

Pierre-Alexandre Vidi, Benjamin R. Chemel, Chang-Deng Hu, and Val J. Watts
Department of Medicinal Chemistry and Molecular Pharmacology, Purdue University, West Lafayette, Indiana
Received March 27, 2008; accepted June 4, 2008

ABSTRACT
Adenosine A_{2A} and dopamine D_2 receptors (A_{2A} and D_2) associate in homo- and heteromeric complexes in the striatum, providing a structural basis for their mutual antagonism. At the cellular level, the portion of receptors engaging in homo- and heteromers, as well as the effect of persistent receptor activation or antagonism on the cell oligomer repertoire, are largely unknown. We have used bimolecular fluorescence complementation (BiFC) to visualize A_{2A} and D_2 oligomerization in the Cath.a differentiated neuronal cell model. Receptor fusions to BiFC fluorescent protein fragments retained their function when expressed alone or in A_{2A}/A_{2A}, D_2/D_2, and A_{2A}/D_2 BiFC pairs. Robust fluorescence complementation reflecting A_{2A}/D_2 heteromers was detected at the cell membrane as well as in endosomes. In contrast, weaker BiFC signals, largely confined to intracellular domains, were detected with A_{2A}/dopamine D_1 BiFC pairs. Multicolor BiFC was used to simultaneously visualize A_{2A} and D_2 homo- and heteromers in living cells and to examine drug-induced changes in receptor oligomers. Prolonged D_2 stimulation with quinpirole lead to the internalization of D_2/D_2 and A_{2A}/D_2 oligomers and resulted in decreased A_{2A}/D_2 relative to A_{2A}/A_{2A} oligomer formation. Opposing effects were observed in cells treated with D_2 antagonists or with the A_{2A} agonist 5′-*N*-methylcarboxamidoadenosine (MECA). Subsequent radioreceptor binding analysis indicated that the drug-induced changes in oligomer formation were not readily explained by alterations in receptor density. These observations support the hypothesis that long-term drug exposure differentially alters A_{2A}/D_2 receptor oligomerization and provide the first demonstration for the use of BiFC to monitor drug-modulated GPCR oligomerization.

A growing number of G protein-coupled receptors (GPCRs) have been shown to exist as oligomers with unique functional properties and physiological relevance (Pin et al., 2007). Evidence suggests that A_{2A} and D_2 form receptor heteromers. Both receptors are highly expressed in the striatum, where they colocalize on spiny neurons (Fink et al., 1992). The receptors have opposing actions on adenylyl cyclase activity, through coupling to $G\alpha_s$ (A_{2A}) or $G\alpha_{i/o}$ (D_2) proteins. Biochemical and behavioral evidence also indicates antagonistic A_{2A}/D_2 interactions (Ferre et al., 1991; Agnati et al., 2003; Fuxe et al., 2007). Moreover, persistent D_2 activation sensitizes A_{2A} receptor-stimulated cAMP accumulation (Vortherms and Watts, 2004). A_{2A} and D_2 have been shown to oligomerize in resonance energy transfer as well as coimmunoprecipitation experiments (Hillion et al., 2002; Canals et al., 2003; Kamiya et al., 2003). Therefore, a direct A_{2A}/D_2 interaction may account for the antagonism between the two receptors. In addition to forming heteromers, A_{2A} and D_2 also exist as homomers (Lee et al., 2000; Armstrong and Strange, 2001; Gazi et al., 2003; Canals et al., 2004; Guo et al., 2005). The stoichiometry of A_{2A} and D_2 in A_{2A}/D_2 heteromers is unknown, as is the relative proportion of A_{2A} and D_2 recep-

This project was funded by Purdue University and by National Institute of Mental Health grant MH060397 (to V.J.W.).
Article, publication date, and citation information can be found at http://molpharm.aspetjournals.org.
doi:10.1124/mol.108.047472.
[S] The online version of this article (available at http://molpharm.aspetjournals.org) contains supplemental material.

ABBREVIATIONS: GPCR, G protein-coupled receptor; BiFC, bimolecular fluorescence complementation; CAD, Cath.a differentiated; HA, hemagglutinin; YFP, yellow fluorescent protein; V, Venus; C, Cerulean; VN, Venus N-terminal fragment; CN, Cerulean N-terminal fragment; VC, Venus C-terminal fragment; CC, Cerulean C-terminal fragment; D_{2L}, long isoform of the dopamine D_2 receptor; MECA, 5′-*N*-Methylcarboxamidoadenosine; CGS15943, 9-chloro-2-(2-furyl)(1,2,4)triazolo(1,5-c)quinazolin-5-amine; Ro 20-1724, 4-(3-butoxy-4-methoxybenzyl)imidazolidin-2-one; ZM 241-385, 4-(2[7-amino-2-(2-furyl)[1,2,4]triazolo[2,3-*a*][1,3,5]triazin-5-ylamino]ethyl)-phenol; ANOVA, analysis of variance; HEK, human embryonic kidney; ER, endoplasmic reticulum.

tors engaging in hetero- or in homomers (or existing as monomeric receptors). Although A_{2A} and D_2 homo- and heteromerization was shown to be constitutive and was not affected by acute receptor activation (Canals et al., 2003; Gazi et al., 2003; Canals et al., 2004), the effect of persistent receptor activation or antagonism on the relative homo-/heteromer population has not been investigated.

Bimolecular fluorescence complementation (BiFC) is an emerging technique to monitor protein-protein interactions (Hu et al., 2002; Shyu et al., 2006). Whereas most currently available techniques are restricted to the detection of two interacting proteins, multicolor BiFC (i.e., the reconstitution of distinct spectral GFP variants) allows the simultaneous detection of two distinct protein-protein interactions in living cells (Hu and Kerppola, 2003). We have applied multicolor BiFC to simultaneously visualize A_{2A}/D_2 heteromers and A_{2A} homomers in the Cath.a differentiated (CAD) neuronal cell model (Qi et al., 1997). The results indicate that A_{2A}/D_2 heteromers coexist and colocalize with A_{2A} homomers. Prolonged (18-h) treatment with the selective D_2 agonist quinpirole or the D_2 antagonist sulpiride had opposing effects on the proportion of A_{2A}/D_2 heteromers relative to A_{2A} homomers. These observations have clinical implications in the management of Parkinson's disease and schizophrenia, which rely on long-term treatment with drugs targeting dopamine receptors.

Materials and Methods

Materials. D_{2L}, A_{2A}, and D_1 cDNAs were obtained from the Missouri S&T cDNA Resource Center. Growth media and reagents (unless otherwise stated) were purchased from Sigma-Aldrich (St. Louis, MO). [^{3}H]cAMP (25 Ci/mmol) was purchased from PerkinElmer Life and Analytical Sciences (Waltham, MA). [^{3}H]Spiperone (85 Ci/mmol) was from GE Healthcare (Chalfont St. Giles, Buckinghamshire, UK).

Cell Culture. CAD cells were maintained as described previously (Vortherms and Watts, 2004).

Expression Vectors. Full-length human D_{2L}, A_{2A}, or D_1 cDNAs were amplified by polymerase chain reaction using oligonucleotides incorporating EcoRI and XbaI or XhoI restriction sites and omitting stop codons. Polymerase chain reaction fragments digested with EcoRI/XbaI or EcoRI/XhoI were ligated into the corresponding sites from pBiFC vectors (Shyu et al., 2006). These vectors contain fragments from the yellow Venus [V (Nagai et al., 2002)] or the cyan Cerulean [C (Rizzo et al., 2004)] enhanced fluorescent proteins. N-Terminal fragments (VN or CN) include residues 1 to 172, whereas C-terminal fragments (VC or CC) include residues 155 to 238. Cloning into pBiFC vectors incorporates MYC (pBiFC-VN), HA (pBiFC-VC and pBiFC-CC), or FLAG (pBiFC-CN) N-terminal epitope tags to the fusion proteins to ease their detection. Receptor fusions to Venus or Cerulean were obtained by swapping BiFC fragments with Venus or Cerulean coding sequences. Constructs were verified by DNA sequencing.

Imaging and Image Analysis. CAD cells were grown to 70% confluence in four-well Lab-Tek coverslips (Nalge Nunc International, Rochester, NY) and transfected using 1 μl/well Lipofectamine 2000 (Invitrogen, Carlsbad, CA), according to the manufacturer's recommendations. DNA amounts per well were 500 ng (D_{2L} and D_1 constructs), 200 ng (A_{2A}-VN), 100 ng (A_{2A}-CC, A_{2A}-CN), or 20 ng (mCherry-Mem, YFP-Endo, YFP-Golgi, and YFP-ER). Twenty-four hours after transfection, the growth media was replaced with phosphate-buffered saline, and images were captured using a charge-coupled device camera mounted on a TE2000-U inverted fluorescence microscope (Nikon Instruments Inc., Melville, NY) equipped with a 100-W mercury lamp and band-pass filters (Chroma, Rockingham, VT) for Venus (excitation at 500/20 nm; emission at 535/30 nm), Cerulean (excitation at 430/25 nm; emission at 470/30 nm), or mCherry (excitation at 572 nm/23 nm). Fluorescent images were acquired using the MetaMorph software (Molecular Devices, Sunnyvale, CA) and AutoDeblur (MediaCybernetics, Bethesda, MD) was used for three-dimensional deconvolution. Blind selection and analysis of the cells avoided experimental bias. Quantification of BiFC signals was performed as described previously (Hu et al., 2002), using the ImageJ software (http://rsb.info.nih.gov/ij/). Stacks of fluorescent images were analyzed as follows. Background fluorescence intensities were determined by measuring areas devoid of cells and were subtracted from each pixel intensity measurement. After background removal, pixel intensities were scaled by a factor equal to the inverse of the exposure time. Images from the mCherry-Mem membrane marker were used to select cells for analysis and to normalize BiFC signals. As an approximation of plasma membrane signals, maximal pixel intensities along lines traced across plasma membranes were measured. Intracellular signals were measured by tracing regions of interest and determining average pixel intensities. Cells with saturated signals, as well as cells with signals lower than 1.5 times background values, were not considered for analysis. Because Venus/mCherry fluorescence ratios exhibited non-Gaussian distributions, median values were calculated and averaged between different experiments. In multicolor BiFC experiments, median Venus/Cerulean fluorescence ratios were measured. For each condition, approximately 40 cells were analyzed. Median values from at least three independent experiments were averaged and used for statistical analysis.

Fluorescence Measurement in Cell Suspensions. CAD cells were grown in 12-well plates, transfected as above, suspended in phosphate-buffered saline, and transferred into 96-well plates (40 μg protein/well; Nalge Nunc International). Cerulean and Venus fluorescence were measured with a Fusion plate reader (Packard, Waltham, MA) using 430/25 nm and 500/20 nm excitation as well as 470/30 nm and 535/30 nm emission fillers, respectively. Background from mock-transfected cells was subtracted from fluorescent signals. Bleed-through and cross-talk coefficients for Cerulean and Venus channels were calculated with cells expressing either V or C (or corresponding BiFC pairs). The C/V fluorescence ratio (noted x coefficient) in cells expressing only Venus was 0.00005 ± 0.00002 ($n = 7$), x in cells expressing VN/CC BiFC fragments was 0.00276 ± 0.00065 ($n = 5$), and the V/C fluorescence ratio (y coefficient) in cells expressing Cerulean was 0.00256 ± 0.00018 ($n = 7$). Corrected Venus (V_{cor}) and Cerulean (C_{cor}) signals were calculated using the equations $V_{cor} = (V - yC)/1 - xy$ and $C_{cor} = (C - xV)/1 - xy$, with V and C indicating the measured Venus and Cerulean fluorescence intensities.

Protein Analysis. Protein concentration was determined using the BCA method (Pierce, Rockford, IL). BiFC-tagged GPCR expression was quantified by dot-blot (Zeder-Lutz et al., 2006). Cell suspensions were lysed with SDS [2% (w/v)], and proteins (5 μg) were spotted onto nitrocellulose membranes using a bio-dot apparatus (Bio-Rad Laboratories, Hercules, CA). Anti-HA (Sigma) or anti-c-MYC (Clontech, Mountain View, CA) mouse antibodies as well as anti-mouse-HRP conjugated antibodies (Bio-Rad Laboratories) were used for immunodetection. Enhanced chemiluminescence signals (ECL+, GE healthcare) were detected and quantified using a Typhoon scanner and the ImageQuant software (Amersham, Chalfont St. Giles, Buckinghamshire, UK).

cAMP Accumulation Assays. Cells were seeded in 48-well plates (approximately 10^5 cells/well) and transiently transfected with 200 ng of plasmid DNA using the Lipofectamine 2000 reagent (0.4 μl/well; Invitrogen). At 24 h after transfection, cells were stimulated for 15 min on ice with drugs diluted in Earle's balanced salt solution assay buffer (Earle's balanced salt solution containing 2% bovine calf serum, 0.025% ascorbic acid, and 15 mM HEPES). In experiments with cells expressing D_{2L} (or D_{2L} fusion proteins), forskolin (30 μM) was used to stimulate adenylyl cyclase. Quinpirole (10 μM) and spiperone (1 μM) were used as D_2-like agonist and antagonist, respectively. 5′-*N*-Methylcarboxamidoadenosine (MECA; 1 μM) and CGS15943 (1 μM) were used as A_{2A} agonist and antagonist, respectively. Dopamine (10 μM) and butaclamol (10 μM) were used as D_1-like agonist and antagonist, respectively. Stimulations were performed in the presence of the phosphodiesterase inhibitors 3-isobutyl-1-methylxanthine (500 μM) or Ro 20-1724 (100 μM for MECA stimulations) and terminated by the addition of 3% trichloroacetic acid. A competitive binding assay was used for cAMP quantification (Vortherms and Watts, 2004).

Radioligand Binding Experiments. Radioreceptor binding experiments were performed as described previously (Watts and Neve, 1996), with minor modifications. A point binding technique was employed to estimate A_{2A} and D_2 receptor densities, using saturating concentrations of radioligand. These concentrations were based on full receptor isotherms, which revealed similar binding properties between the fusion proteins and wild-type receptors (data not shown). Twenty-four hours after transfection and 18 h after drug treatment, cells in 12-well plates were washed and lysed in 1 ml of ice-cold lysis buffer (1 mM HEPES and 2 mM EDTA, pH 7.4) and membranes were collected by centrifugation (10 min at 13,000*g*). Membrane pellets were resuspended by mechanical homogenation in 500 μl of receptor binding buffer (50 mM Tris and 4 mM $MgCl_2$, pH 7.4). Membranes for A_{2A} receptor experiments were treated with 2 U/ml adenosine deaminase (Roche Applied Science, Indianapolis, IN) at 37°C for 30 min to remove endogenous adenosine. Treated membranes (10–20 μg of protein in 100 μl) were added in duplicate to assay tubes to determine total and nonspecific binding (defined by 50 μM adenosine-5′*N*-ethylcarboxamide). All tubes contained [^{3}H]ZM 241-385 (~2.5 nM; American Radioligand Chemicals, St. Louis, MO) in a final volume of 500 μl and were incubated for 1 h at 25°C. D_2 binding experiments were performed in a similar fashion, excluding adenosine deaminase treatment. Total binding at D_2 was determined by incubating 10 to 20 μg of protein (in 100 μl) membrane suspensions with [^{3}H]spiperone (~0.5 nM; Amersham) at 37°C for 30 min in a total volume of 500 μl receptor of binding buffer. Nonspecific binding was defined by using 5 μM (+)-butaclamol. A_{2A} and D_2 binding assays were terminated by filtration onto FB glass fiber plates with ice-cold wash buffer (10 mM Tris and 0.9% NaCl) using a cell harvester (FilterMate; Packard). Radioactivity was determined using a Packard TopCount scintillation counter. Specific binding for each sample was determined as the difference between the average counts for total versus nonspecific binding. The specific binding values were normalized to the amount of protein added per well, as determined by the Pierce BCA Protein Assay. Within an experiment, drug treatments were performed in triplicate, and for each of these, total and nonspecific binding conditions were performed in duplicate.

Statistical Analysis. Statistical analysis was performed using Prism (GraphPad Software Inc., San Diego, CA). Student's *t* test or one-way ANOVA followed by post hoc tests are indicated with the corresponding *p* values in the figure legends. A *p* value < 0.05 was considered significant.

Results and Discussion

A_{2A} and D_{2L} Oligomerization in the CAD Neuronal Cell Model Detected by BiFC. Interactions between A_{2A} and D_{2L} were studied in CAD neuronal cells. Fluorescence resonance energy transfer studies with cells coexpressing A_{2A}-Cerulean and D_{2L}-Venus suggested heteromerization of A_{2A} and D_{2L} in CAD cells (data not shown), consistent with previous reports (Canals et al., 2003; Kamiya et al., 2003). To establish BiFC as a tool to visualize A_{2A}/D_{2L} heteromerization, we engineered A_{2A} and D_{2L} fusions to VN and VC or CN and CC. Function of the BiFC fusion receptors was addressed by measuring cAMP accumulation in response to agonists in cells expressing -VN or -VC receptor fusions or untagged receptors (Fig. 1). Inhibitory effects on adenylyl cyclase were measured in CAD cells expressing D_{2L}, D_{2L}-VN, or D_{2L}-VC. Treatment with the D_2 agonist quinpirole resulted in inhibition of forskolin-stimulated cAMP accumulation, which was

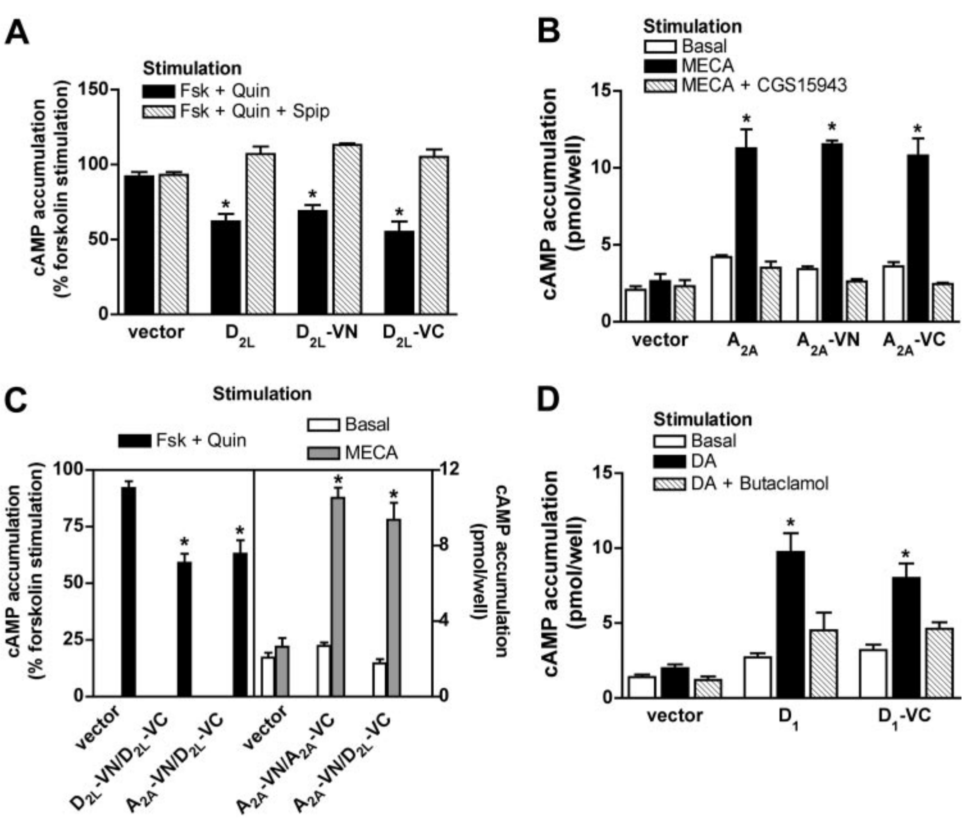

Fig. 1. Functional characterization of receptor-BiFC fragment fusion proteins. A, inhibition of forskolin (Fsk)-stimulated cAMP accumulation was measured in CAD cells expressing D_{2L}, D_{2L}-VN, or D_{2L}-VC after stimulation with quinpirole (Quin, 10 μM) in the absence or presence of spiperone (Spip, 1 μM). B, cAMP accumulation in HEK-293 cells expressing A_{2A}, A_{2A}-VN, or A_{2A}-VC was measured under basal conditions or in the presence of MECA (1 μM) in the absence or presence of CGS15943 (1 μM) as indicated. C, receptor function in cells expressing D_2-VN/D_2-VC, A_{2A}-VN/D_2-VC, or A_{2A}-VN/A_{2A}-VC BiFC pairs. cAMP accumulation was measured in CAD cells as in A for the left panel and in HEK-293 cells as in B for the right panel. D, cAMP accumulation in CAD cells expressing D_1 or D_1-VC under basal conditions or in the presence of dopamine (DA; 10 μM) in the absence or presence of butaclamol (10 μM), as indicated. Data are means ± S.E.M. of at least three experiments assayed in duplicate. *, $p < 0.001$ compared with empty vector transfections (one-way ANOVA followed by Dunnett's post hoc test).

blocked by the addition of the D_2 antagonist spiperone (Fig. 1A). Because CAD cells endogenously express A_{2A} (Vortherms and Watts, 2004), A_{2A}, A_{2A}-VN, or A_{2A}-VC were expressed in HEK-293 cells to verify their function. Short-term activation of A_{2A} receptors with the adenosine analog MECA resulted in increased cAMP accumulation in cells expressing each of the constructs. This effect was blocked by the A_{2A} antagonist CGS15943 (Fig. 1B). Subsequent studies examined agonist responses in cells coexpressing D_{2L}-VN/D_{2L}-VC, A_{2A}-VN/D_{2L}-VC, or A_{2A}-VN/A_{2A}-VC (Fig. 1C). The results of these experiments demonstrated that fluorescence complementation did not disrupt quinpirole- or MECA-stimulated receptor function. Function of the dopamine D_1 receptor (D_1) fusion to VC was also addressed in CAD cells expressing D_1 or D_1-VC. D_1-mediated dopamine stimulation of cAMP accumulation was similar in both transfections and was blocked by the dopamine receptor antagonist butaclamol (Fig. 1D). Together, these results revealed that -VN and -VC fusion receptors retained ligand-dependent function in the conditions tested. Because Cerulean and Venus have virtually identical structures, we assume that the functional data described above are relevant for receptor fusions to both Venus and Cerulean fragments.

Subsequent experiments used the novel BiFC fusion receptors to explore the localization and specificity of fluorescence complementation in CAD cells. Cells coexpressing A_{2A}-VN and D_{2L}-VC exhibited robust Venus fluorescence detected in whole-cell fluorescence measurements (Fig. 2A) or using microscopy (Fig. 2B). Because biochemical evidence suggests a weak A_{2A}/D_1 interaction (Hillion et al., 2002), control experiments in which D_1-VC replaced D_{2L}-VC were used to address the specificity of the fluorescent complementation. Fluorescent signals from cells expressing A_{2A}-VN and D_{2L}-VC were significantly higher than signals in A_{2A}-VN and D_1-VC transfections (Fig. 2, A and B). Analysis of receptor expression levels in dot-blot experiments suggested that this difference was not a result of reduced D_1-VC protein expression levels compared with D_{2L}-VC (Fig. 2C). Likewise, A_{2A}-VN levels were not significantly different when cotransfected with D_{2L}-VC or D_1-VC (data not shown). The localization of the A_{2A}/D_{2L} and A_{2A}/D_1 interactions was then analyzed at the subcellular level. Strong BiFC signals were observed at the plasma membrane in cells expressing A_{2A}-VN and D_{2L}-VC (Fig. 2, B and D). Signals were also detected in intracellular compartments, presumably reflecting receptor internalization or localization at the endoplasmic reticulum (ER). In experiments using A_{2A}-VN and D_1-VC pairs, BiFC signal intensity at the plasma membrane was reduced by more than 60% compared with A_{2A}/D_{2L} signals (Fig. 2, B and D). Cells expressing A_{2A}-VN and D_1-VC seemed to display an increased proportion of intracellular fluorescence (Fig. 2E), suggesting more extensive internalization or less efficient export to the plasma membrane of A_{2A}/D_1, possibly as a consequence of quality-control mechanisms at the endoplasmic reticulum (Bulenger et al., 2005).

A_{2A} and D_{2L} Homo- and Heteromerization Monitored Simultaneously in Living Cells. Multicolor BiFC (Hu and Kerppola, 2003) was used to simultaneously visualize and compare A_{2A}/D_{2L} heteromers and A_{2A} homomers. The D_{2L}-VN construct was cotransfected with A_{2A} fusions to N- and C-terminal fragments of Cerulean (A_{2A}-CN and A_{2A}-CC) in CAD cells. Reconstitution of Venus-like fluorescence was

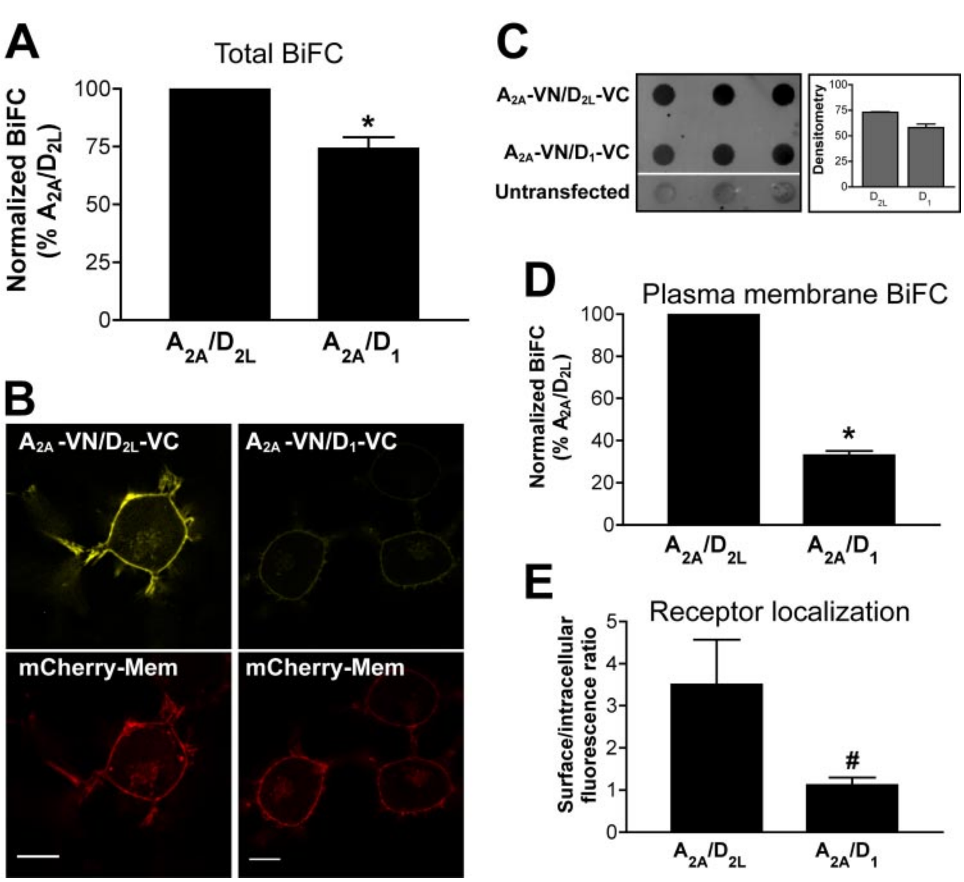

Fig. 2. A_{2A}/D_{2L} and A_{2A}/D_1 oligomers detected with BiFC. A, signals from Venus complementation (VN-VC) in cells transfected with A_{2A}-VN (A_{2A}) and D_{2L}-VC (D_{2L}) or A_{2A}-VN and D_1-VC (D_1) were detected by fluorometry. B, fluorescence in cells expressing A_{2A}-VN, D_{2L}-VC, or D_1-VC and the membrane marker mCherry-Mem was monitored by fluorescence microscopy. C, expression levels of D_{2L}- or D_1-VC fusion proteins were quantified by dot blot using anti-HA antibodies. Densitometry analysis is shown as a mean ± S.E.M from three independent experiments. Surface (plasma membrane) signals (D) and surface/intracellular fluorescence ratios (E) were measured in microscopic images as described under *Materials and Methods*. Scale bar, 10 μm; *, $p < 0.001$ (one-sample t test, n ≥3); #, $p < 0.05$ (unpaired t test, n = 3), compared with A_{2A}-VN/D_{2L}-VC.

indicative of A_{2A}/D_{2L} heteromer formation, whereas Cerulean fluorescence reflected A_{2A} homomerization (Fig. 3A, Supplemental Fig. 1A). Cells imaged by fluorescence microscopy displayed both Venus and Cerulean signals, indicating coexistence of A_{2A}/D_{2L} hetero- and A_{2A} homomers within a cell. Both fluorescent signals largely colocalized at the plasma membrane as well as in intracellular compartments. Similar observations were made with cells transfected with D_{2L}-VN, A_{2A}-CN, and D_{2L}-CC (Supplemental Fig. 1B). Venus (D_{2L}/D_{2L}) and Cerulean (A_{2A}/D_{2L}) fluorescent signals coexisted and largely colocalized at the plasma membrane and in intracellular vesicular structures.

To our knowledge, this is the first study in which multiple GPCR interactions were simultaneously visualized in living cells. The localization of the A_{2A}/D_{2L} oligomer was further addressed by cotransfecting A_{2A}-CN and D_{2L}-CC with three distinct fluorescent markers (Fig. 3B). There was virtually no overlap of A_{2A}-CN/D_{2L}-CC fluorescence with the transmedial Golgi marker (YFP-Golgi; YFP fusion to residues 1–81 of the β1,4-galactosyltransferase). Consistent with recent studies suggesting biogenesis of serotonin 5-HT_{2C} homomers, β_2 adrenergic receptor homomers, and D_1/D_2 heteromers at the ER (Salahpour et al., 2004; So et al., 2005; Herrick-Davis et al., 2006), A_{2A}-CN/D_{2L}-CC fluorescence showed a moderate level of overlap with the ER marker (YFP-ER; YFP fused to the ER targeting sequence of calreticulin and the KEDL ER retrieval sequence). There was also significant overlap of A_{2A}/D_{2L} and structures labeled with the endosomal marker RhoB (Adamson et al., 1992) fused to YFP (YFP-Endo), suggesting trafficking of A_{2A}/D_{2L} heteromers through early endosomes as reported for a number of GPCRs including D_2 (Seachrist and Ferguson, 2003). Collectively, these results indicate proper trafficking of BiFC-tagged fusion receptors.

Effect of Ligands on Receptor Localization. Having established multicolor BiFC as a tool to detect receptor homo- and heteromers in a neuronal model, subsequent microscopic studies were designed to examine the effect of long term D_2 agonist and antagonist treatments on D_{2L} and A_{2A} homo- and heteromer localization. In cells expressing D_{2L}-VN, A_{2A}-CN, and A_{2A}-CC, 18-h quinpirole treatment resulted in a decreased ratio of surface to intracellular Venus (A_{2A}/D_{2L}) signals (Fig. 3C and Supplemental Fig. 1A). This effect was blocked by coapplication of the D_2 antagonist sulpiride. In reciprocal experiments, cells transfected with D_{2L}-VN, A_{2A}-CN, and D_{2L}-CC revealed a similar reduction of surface to intracellular fluorescence for BiFC signals of Cerulean (A_{2A}/D_{2L}) and Venus (D_{2L}/D_{2L}) after quinpirole treatment (Fig. 3C and Supplemental Fig. 1B). Sulpiride blocked the effect of quinpirole on A_{2A}/D_{2L} fluorescence and seemed to increase the plasma membrane localization for D_{2L}/D_{2L}, possibly by reducing constitutive activity of D_{2L}/D_{2L} oligomers. These observations are consistent with a quinpirole-induced internalization of D_{2L}/D_{2L} homomers and A_{2A}/D_{2L} heteromers (Hillion et al., 2002).

Effect of Ligands on Receptor Oligomerization. We examined the effect of persistent A_{2A} and D_{2L} stimulation on the relative proportion of receptor homo- and heteromer formation. Cells expressing D_{2L}-VN, A_{2A}-CN, and A_{2A}-CC treated with quinpirole for 18 h displayed decreased Venus over Cerulean fluorescence at the plasma membrane compared with vehicle-treated cells, indicating decreased A_{2A}/D_{2L} relative to A_{2A} oligomer formation (Fig. 3, D and E). The inclusion of sulpiride prevented this change and reversed the fluorescence ratio. Intracellular fluorescence was similarly influenced by the drug treatments, indicating that changes of fluorescence intensity at the plasma membrane did not solely result from altered receptor trafficking. To validate the microscopic analysis, nonbiased whole-cell fluorescence measurements were taken (Fig. 3F). These studies also revealed a decrease in Venus (A_{2A}/D_{2L}) over Cerulean (A_{2A}/A_{2A}) fluorescence consequent to quinpirole treatment. The effect of quinpirole was reversed by the D_2 antagonists spiperone or sulpiride. Furthermore, D_2 antagonists alone caused a marked increase of Venus over Cerulean fluorescence. This increase was similar to that observed when antagonists were coapplied with quinpirole. No significant effect of the quinpirole treatment was observed in control experiments where the D_1 receptor replaced D_{2L} (data not shown). In experiments with cells expressing D_{2L}-VN, A_{2A}-CN, and D_{2L}-CC, prolonged quinpirole treatment led to increased Venus over Cerulean fluorescence (Supplemental Fig. 2), indicative of increased D_{2L}/D_{2L} over A_{2A}/D_{2L} oligomerization.

The effect of persistent A_{2A} stimulation on A_{2A} homo- and A_{2A}/D_{2L} heteromerization was addressed by treating cells expressing D_{2L}-VN, A_{2A}-CN, and A_{2A}-CC with the adenosine receptor agonist MECA (Fig. 3F). Treatment with MECA increased the proportion of A_{2A}/D_{2L} (Venus) over A_{2A}/A_{2A} (Cerulean) oligomers and this effect was blocked by coapplication of the adenosine antagonist CGS15943. When applied alone, CGS15943 had no effect on BiFC fluorescence. Control experiments determined that the D_2 and A_{2A} ligands tested did not emit fluorescence when excited with wavelengths corresponding to Venus or Cerulean excitation (data not shown).

The differential effect of ligands on BiFC fluorescence may reflect ligand-dependent alterations of receptor density. Thus, we measured D_2 and A_{2A} receptor levels in cells transfected with D_{2L}-VN, A_{2A}-CN, and A_{2A}-CC using single-point radioreceptor binding assays. Both quinpirole and sulpiride treatments lead to increased D_2 receptor density, whereas MECA and CGS15943 had no effect on D_2 expression (Table 1). An up-regulation of D_{2L}-VN protein levels after quinpirole, sulpiride, or spiperone treatments was also revealed in dot-blot experiments (data not shown). These results are

TABLE 1

D_2 and A_{2A} receptor density following prolonged ligand exposure in CAD cells expressing D_{2L}-VN, A_{2A}-CN, and A_{2A}-CC

D_{2L}-VN density was estimated in single point binding experiments using [^{3}H]spiperone; A_{2A}-CN and A_{2A}-CC density was estimated in single point binding experiments using [^{3}H]ZM 241–385. Data are means ± S.E.M. of at least four independent experiments assayed in triplicate. Receptor density in vehicle-treated cells was 2560 ± 260 (D_{2L}, n = 10) and 5410 ± 520 (A_{2A}, n = 5) fmol/mg protein. Untransfected cells did not exhibit detectable D_2 and A_{2A} binding levels in this single point assay.

Ligand	Receptor Density	
	D_2	A_{2A}
	% vehicle	
Quinpirole (10 μM)	140 ± 5*	128 ± 4*
S-(−)-Sulpiride (10 μM)	172 ± 10*	124 ± 7*#
MECA (10 μM)	96 ± 7	122 ± 1*#
CGS15943 (10 μM)	85 ± 9	N.D.

N.D., not determined.
* $P < 0.05$, one-sample t test.
\# $P < 0.05$, unpaired two-tailed t test compared with D_2.

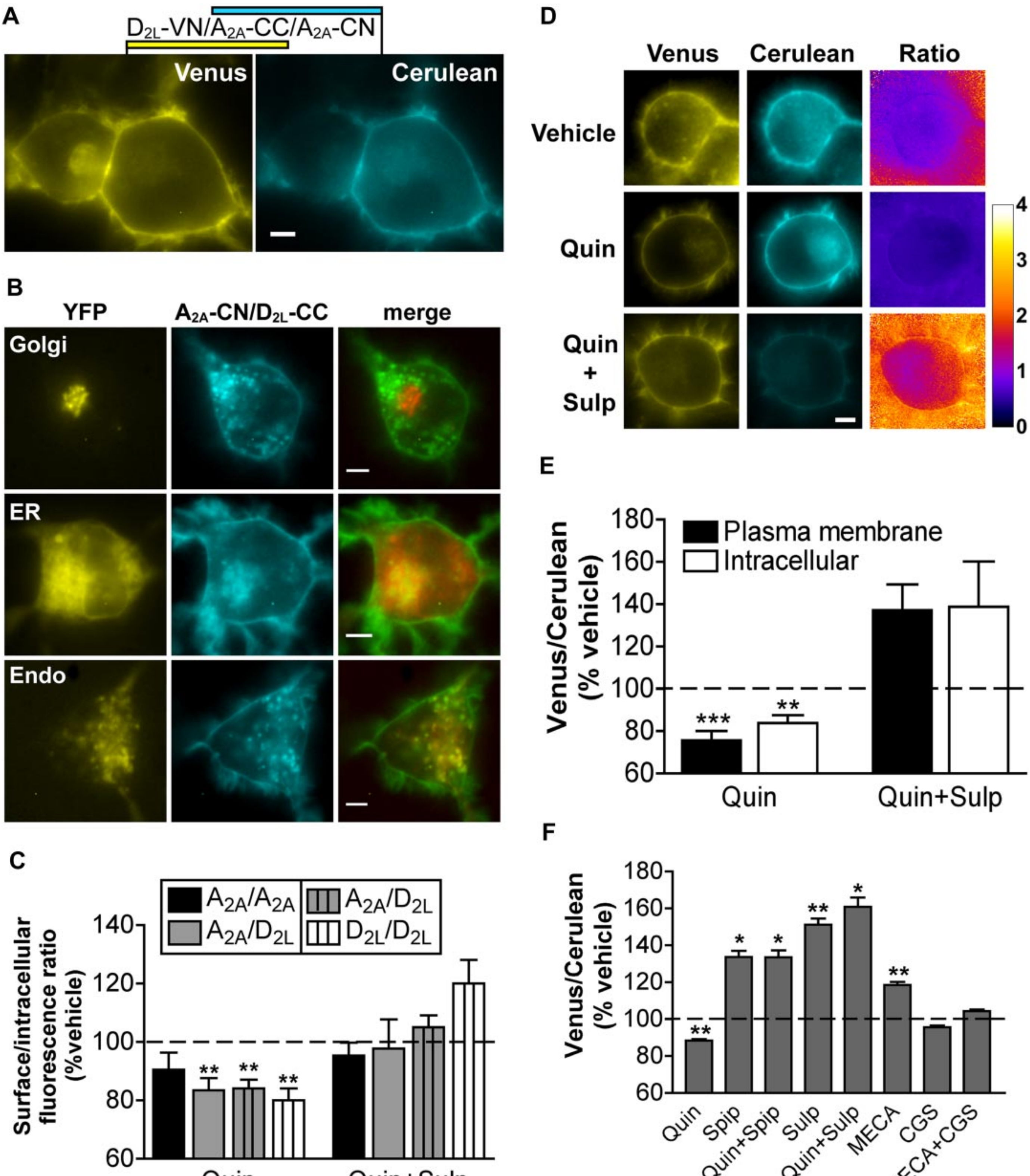

Fig. 3. Effect of ligands on A_{2A} and D_{2L} homo- and heteromer formation and trafficking. A, complemented Venus and Cerulean fluorescence in cells expressing D_{2L}-VN, A_{2A}-CN, and A_{2A}-CC was monitored by fluorescence microscopy. B, localization of intracellular A_{2A}/D_{2L} heteromers. Microscopic images from cells cotransfected with A_{2A}-CN, D_{2L}-CC (in cyan), and either YFP-Golgi, YFP-ER, or YFP-Endo (in yellow). Merged images are shown with YFP signals in red and CN/CC signals in green. Overlapping signals are in yellow. C, internalization of A_{2A} and D_{2L} homo- and heteromers after prolonged (18 h) D_{2L} activation with quinpirole (Quin, 10 μM) in the absence or presence of sulpiride (Sulp, 10 μM). Surface over intracellular fluorescence was measured in cells transfected with D_{2L}-VN, A_{2A}-CN, and A_{2A}-CC (solid bars) or with D_{2L}-VN, A_{2A}-CN, and D_{2L}-CC (striped bars). D and E, relative oligomer formation after prolonged exposure to quinpirole or sulpiride in cells expressing D_{2L}-VN, A_{2A}-CN, and A_{2A}-CC. D, ratiometric images (Ratio) represent Venus over Cerulean signals and are displayed in pseudocolors. The corresponding intensity scale is shown. E, fluorescent signals at the plasma membrane or in intracellular compartments were measured and expressed as Venus/Cerulean fluorescence ratio. Note: portions of data used for C (D_{2L}-VN, A_{2A}-CN, and A_{2A}-CC transfected cells) were also used in E. F, whole-cell fluorescence after treatment with quinpirole (10 μM), spiperone (Spip, 1 μM), sulpiride (10 μM), MECA (10 μM), or CGS15943 (CGS, 10 μM) was measured by fluorometry. Scale bars: 5 μm. *, $p < 0.05$; **, $p < 0.01$; ***, $p < 0.001$ (compared with vehicle, one-sample t test, n = 3–11).

consistent with previous reports (Filtz et al., 1994; Zhang et al., 1994; Starr et al., 1995) and likely reflect a pharmacological chaperone effect (Bernier et al., 2004; Conn et al., 2007) on D_2 by its ligands, as previously reported for δ opioid (Petäjä-Repo et al., 2002) and D_4 dopamine (Van Craenenbroeck et al., 2005) receptors. Although previous reports failed to observe an effect of prolonged (14 h) A_{2A} stimulation on A_{2A} expression (Chern et al., 1993), MECA treatment increased A_{2A} receptor density (Table 1). Unexpectedly, both quinpirole and sulpiride also caused a significant increase in A_{2A} density in D_{2L}-VN, A_{2A}-CN, and A_{2A}-CC transfected cells (Table 1). The mechanisms underlying the modest up-regulation of A_{2A} by MECA, quinpirole, and sulpiride are not clear and probably involve multiple pathways. For example, prolonged stimulation or antagonism of A_{2A} or D_2 receptors may lead to changes in intracellular cAMP concentrations and as a result modify extracellular adenosine levels altering A_{2A} density (Do et al., 2007). In addition, pharmacological chaperone effects of D_2 ligands may help A_{2A}/D_2 heteromers pass quality control at the ER (Bulenger et al., 2005) and therefore promote both D_2 and A_{2A} expression. These possibilities will be explored in future experiments.

The drug-induced up-regulation of receptor levels may (at least partially) account for the change in receptor oligomerization monitored with BiFC. The increased A_{2A}/D_{2L} relative to A_{2A}/A_{2A} BiFC signals after prolonged D_2 antagonism may be consistent with greater D_2 versus A_{2A} up-regulation by sulpiride (1.72- and 1.24-fold over vehicle, respectively; Table 1). In contrast, increased A_{2A}/D_{2L} relative to A_{2A}/A_{2A} oligomerization resulting from persistent A_{2A} stimulation was accompanied with increased A_{2A} in the absence of D_2 level changes; inconsistent with BiFC signals simply reflecting receptor densities. Furthermore, both sulpiride and quinpirole increased D_2 and A_{2A} levels but had opposing effects on receptor oligomerization. These observations suggest that a quinpirole-induced up-regulation of D_2 and A_{2A} was not responsible for the observed reduction of A_{2A}/D_{2L} relative to A_{2A}/A_{2A} oligomers. Rather, we propose that ligand-mediated changes in receptor conformation and/or microenvironment localization may influence the formation of receptor oligomers. For example, the activation of D_2 may result in a stronger propensity to form homomers and/or decrease D_2 affinity for A_{2A} receptors by modifying the interaction interface. Consistent with this hypothesis is the observation that prolonged quinpirole treatment lead to increased D_{2L}/D_{2L} relative to A_{2A}/D_{2L} (Supplemental Fig. 2) and decreased A_{2A}/D_{2L} relative to A_{2A}/A_{2A} oligomer formation (Fig. 3).

We used a novel approach to study GPCR interactions and observed ligand-mediated effects on oligomer formation (Pfleger and Eidne, 2005). GPCR oligomerization has been proposed to be altered in pathogenic situations or by long-term drug administration such as in Parkinson's disease therapies (Javitch, 2004; Fuxe et al., 2007). Therapies for Parkinson's disease largely rely on long-term dopamine receptor stimulation with L-DOPA to compensate for the loss of striatal dopaminergic neurons and are often accompanied with dyskinesias. A_{2A} antagonists have recently been applied with reduced L-DOPA doses in clinical studies and were shown to prevent and alleviate L-DOPA-induced dyskinesias (Schwarzschild et al., 2006; Morelli et al., 2007). Although a precise understanding of the molecular mechanisms underlying this adjunctive therapy are lacking, it has been proposed that long-term L-DOPA treatment may alter A_{2A} and D_2 homo- and heteromerization on striatal neurons (Antonelli et al., 2006). The present studies provide support for that model. In particular, the D_2 agonist-induced decrease in A_{2A}/D_2 heteromers relative to A_{2A} homomers may alleviate the constitutive D_2 antagonism of A_{2A} signaling. Such an increase in A_{2A} signaling may play a role in the sensitization of A_{2A}-mediated cAMP accumulation after activation of D_2 receptors (Vortherms and Watts, 2004). Moreover, a D_2 agonist-induced enhancement of A_{2A} signaling also provides a molecular explanation for the beneficial effects of A_{2A} antagonists in L-DOPA-induced dyskinesias (Morelli et al., 2007). These observations and the results in the present study highlight the applicability of multicolor BiFC as a novel approach to examine physiologically relevant GPCR interactions. Moreover, it may offer a novel technique for screening drugs that target GPCR oligomers.

Acknowledgments

We thank John Shyu, Julie A. Stacey, and Jason Conley (Purdue University, West Lafayette, IN) for providing invaluable advice and comments. The mCherry-Mem, YFP-Endo, YFP-ER, and YFP-Golgi constructs were gifts from Dr. C. Berlot (Weis Center for Research, Danville, PA).

References

Adamson P, Paterson HF, and Hall A (1992) Intracellular localization of the P21rho proteins. *J Cell Biol* **119:**617–627.

Agnati LF, Ferré S, Lluis C, Franco R, and Fuxe K (2003) Molecular mechanisms and therapeutical implications of intramembrane receptor/receptor interactions among heptahelical receptors with examples from the striatopallidal GABA neurons. *Pharmacol Rev* **55:**509–550.

Antonelli T, Fuxe K, Agnati L, Mazzoni E, Tanganelli S, Tomasini MC, and Ferraro L (2006) Experimental studies and theoretical aspects on A2A/D2 receptor interactions in a model of Parkinson's disease. Relevance for L-dopa induced dyskinesias. *J Neurol Sci* **248:**16–22.

Armstrong D and Strange PG (2001) Dopamine D2 receptor dimer formation: evidence from ligand binding. *J Biol Chem* **276**:22621–22629.

Bernier V, Bichet DG, and Bouvier M (2004) Pharmacological chaperone action on G-protein-coupled receptors. *Curr Opin Pharmacol* **4:**528–533.

Bulenger S, Marullo S, and Bouvier M (2005) Emerging role of homo- and heterodimerization in G-protein-coupled receptor biosynthesis and maturation. *Trends Pharmacol Sci* **26:**131–137.

Canals M, Burgueño J, Marcellino D, Cabello N, Canela EI, Mallol J, Agnati L, Ferré S, Bouvier M, Fuxe K, et al. (2004) Homodimerization of adenosine A2A receptors: qualitative and quantitative assessment by fluorescence and bioluminescence energy transfer. *J Neurochem* **88:**726–734.

Canals M, Marcellino D, Fanelli F, Ciruela F, de Benedetti P, Goldberg SR, Neve K, Fuxe K, Agnati LF, Woods AS, et al. (2003) Adenosine A2A-dopamine D2 receptor-receptor heteromerization: qualitative and quantitative assessment by fluorescence and bioluminescence energy transfer. *J Biol Chem* **278:**46741–46749.

Chern Y, Lai HL, Fong JC, and Liang Y (1993) Multiple mechanisms for desensitization of A2a adenosine receptor-mediated cAMP elevation in rat pheochromocytoma PC12 cells. *Mol Pharmacol* **44:**950–958.

Conn PM, Ulloa-Aguirre A, Ito J, and Janovick JA (2007) G Protein-Coupled Receptor Trafficking in Health and Disease: Lessons Learned to Prepare for Therapeutic Mutant Rescue in Vivo. *Pharmacol Rev* **59:**225–250.

Do T, Sun Q, Beuve A, and Kuzhikandathil EV (2007) Extracellular cAMP inhibits D1 dopamine receptor expression in CAD catecholaminergic cells via A2a adenosine receptors. *J Neurochem* **101:**619–631.

Ferre S, von Euler G, Johansson B, Fredholm BB, and Fuxe K (1991) Stimulation of high-affinity adenosine A2 receptors decreases the affinity of dopamine D2 receptors in rat striatal membranes. *Proc Natl Acad Sci U S A* **88:**7238–7241.

Filtz TM, Guan W, Artymyshyn RP, Facheco M, Ford C, and Molinoff PB (1994) Mechanisms of up-regulation of D2L dopamine receptors by agonists and antagonists in transfected HEK-293 cells. *J Pharmacol Exp Ther* **271:**1574–1582.

Fink JS, Weaver DR, Rivkees SA, Peterfreund RA, Pollack AE, Adler EM, and Reppert SM (1992) Molecular cloning of the rat A2 adenosine receptor: selective co-expression with D2 dopamine receptors in rat striatum. *Brain Res Mol Brain Res* **14:**186–195.

Fuxe K, Canals M, Torvinen M, Marcellino D, Terasmaa A, Genedani S, Leo G, Guidolin D, Diaz-Cabiale Z, Rivera A, et al. (2007) Intramembrane receptor-receptor interactions: a novel principle in molecular medicine. *J Neural Transm* **114:**49–75.

Gazi L, López-Giménez JF, Rüdiger MP, and Strange PG (2003) Constitutive oligomerization of human D2 dopamine receptors expressed in Spodoptera frugiperda 9 (Sf9) and in HEK293 cells. Analysis using co-immunoprecipitation and time-resolved fluorescence resonance energy transfer. *Eur J Biochem* **270:**3928–3938.

Guo W, Shi L, Filizola M, Weinstein H, and Javitch JA (2005) Crosstalk in G protein-coupled receptors: changes at the transmembrane homodimer interface determine activation. *Proc Natl Acad Sci U S A* **102:**17495–17500.

Herrick-Davis K, Weaver BA, Grinde E, and Mazurkiewicz JE (2006) Serotonin 5-HT2C receptor homodimer biogenesis in the endoplasmic reticulum: real-time visualization with confocal fluorescence resonance energy transfer. *J Biol Chem* **281:**27109–27116.

Hillion J, Canals M, Torvinen M, Casado V, Scott R, Terasmaa A, Hansson A, Watson S, Olah ME, Mallol J, et al. (2002) Coaggregation, cointernalization, and codesensitization of adenosine A2A receptors and dopamine D2 receptors. *J Biol Chem* **277:**18091–18097.

Hu CD, Chinenov Y, and Kerppola TK (2002) Visualization of interactions among bZIP and Rel family proteins in living cells using bimolecular fluorescence complementation. *Mol Cell* **9:**789–798.

Hu CD and Kerppola TK (2003) Simultaneous visualization of multiple protein interactions in living cells using multicolor fluorescence complementation analysis. *Nat Biotechnol* **21:**539–545.

Javitch JA (2004) The ants go marching two by two: oligomeric structure of G-protein-coupled receptors. *Mol Pharmacol* **66:**1077–1082.

Kamiya T, Saitoh O, Yoshioka K, and Nakata H (2003) Oligomerization of adenosine A2A and dopamine D2 receptors in living cells. *Biochem Biophys Res Commun* **306:**544–549.

Lee SP, O'Dowd BF, Ng GY, Varghese G, Akil H, Mansour A, Nguyen T, and George SR (2000) Inhibition of cell surface expression by mutant receptors demonstrates that D2 dopamine receptors exist as oligomers in the cell. *Mol Pharmacol* **58:**120–128.

Morelli M, Di Paolo T, Wardas J, Calon F, Xiao D, and Schwarzschild MA (2007) Role of adenosine A2A receptors in parkinsonian motor impairment and *l*-DOPA-induced motor complications. *Prog Neurobiol* **83:**293–309.

Nagai T, Ibata K, Park ES, Kubota M, Mikoshiba K, and Miyawaki A (2002) A variant of yellow fluorescent protein with fast and efficient maturation for cell-biological applications. *Nat Biotechnol* **20:**87–90.

Petäjä-Repo UE, Hogue M, Bhalla S, Laperrière A, Morello JP, and Bouvier M (2002) Ligands act as pharmacological chaperones and increase the efficiency of delta opioid receptor maturation. *EMBO J* **21:**1628–1637.

Pfleger KD and Eidne KA (2005) Monitoring the formation of dynamic G-protein-coupled receptor-protein complexes in living cells. *Biochem J* **385:**625–637.

Pin JP, Neubig R, Bouvier M, Devi L, Filizola M, Javitch JA, Lohse MJ, Milligan G, Palczewski K, Parmentier M, et al. (2007) International Union of Basic and Clinical Pharmacology. LXVII. Recommendations for the recognition and nomenclature of G protein-coupled receptor heteromultimers. *Pharmacol Rev* **59:**5–13.

Qi Y, Wang JK, McMillian M, and Chikaraishi DM (1997) Characterization of a CNS cell line, CAD, in which morphological differentiation is initiated by serum deprivation. *J Neurosci* **17:**1217–1225.

Rizzo MA, Springer GH, Granada B, and Piston DW (2004) An improved cyan fluorescent protein variant useful for FRET. *Nat Biotechnol* **22:**445–449.

Salahpour A, Angers S, Mercier JF, Lagacé M, Marullo S, and Bouvier M (2004) Homodimerization of the β_2-adrenergic receptor as a prerequisite for cell surface targeting. *J Biol Chem* **279:**33390–33397.

Schwarzschild MA, Agnati L, Fuxe K, Chen JF, and Morelli M (2006) Targeting adenosine A2A receptors in Parkinson's disease. *Trends Neurosci* **29:**647–654.

Seachrist JL and Ferguson SS (2003) Regulation of G protein-coupled receptor endocytosis and trafficking by Rab GTPases. *Life Sci* **74:**225–235.

Shyu YJ, Liu H, Deng X, and Hu CD (2006) Identification of new fluorescent protein fragments for bimolecular fluorescence complementation analysis under physiological conditions. *Biotechniques* **40:**61–66.

So CH, Varghese G, Curley KJ, Kong MM, Alijaniaram M, Ji X, Nguyen T, O'Dowd BF, and George SR (2005) D1 and D2 dopamine receptors form heterooligomers and cointernalize after selective activation of either receptor. *Mol Pharmacol* **68:**568–578.

Starr S, Kozell LB, and Neve KA (1995) Drug-induced up-regulation of dopamine D2 receptors on cultured cells. *J Neurochem* **65:**569–577.

Van Craenenbroeck K, Clark SD, Cox MJ, Oak JN, Liu F, and Van Tol HH (2005) Folding efficiency is rate-limiting in dopamine D4 receptor biogenesis. *J Biol Chem* **280:**19350–19357.

Vortherms TA and Watts VJ (2004) Sensitization of neuronal A2A adenosine receptors after persistent D2 dopamine receptor activation. *J Pharmacol Exp Ther* **308:**221–227.

Watts VJ and Neve KA (1996) Sensitization of endogenous and recombinant adenylate cyclase by activation of D2 dopamine receptors. *Mol Pharmacol* **50:**966–976.

Zeder-Lutz G, Cherouati N, Reinhart C, Pattus F, and Wagner R (2006) Dot-blot immunodetection as a versatile and high-throughput assay to evaluate recombinant GPCRs produced in the yeast Pichia pastoris. *Protein Expr Purif* **50:**118–127.

Zhang LJ, Lachowicz JE, and Sibley DR (1994) The D2S and D2L dopamine receptor isoforms are differentially regulated in Chinese hamster ovary cells. *Mol Pharmacol* **45:**878–889.

Address correspondence to: Val J. Watts, Dept. of Medicinal Chemistry and Molecular Pharmacology, Purdue University, 575 Stadium Mall Drive, West Lafayette, IN 47907. E-mail: wattsv@purdue.edu.